A Wavelet-Chaos Methodology for Analysis of EEGs and EEG Subbands to Detect Seizure and Epilepsy

Hojjat Adeli*, *Member, IEEE*, Samanwoy Ghosh-Dastidar, and Nahid Dadmehr

***Abstract*—A wavelet-chaos methodology is presented for analysis of EEGs and *delta*, *theta*, *alpha*, *beta*, and *gamma* subbands of EEGs for detection of seizure and epilepsy. The nonlinear dynamics of the original EEGs are quantified in the form of the correlation dimension (CD, representing system complexity) and the largest Lyapunov exponent (LLE, representing system chaoticity). The new wavelet-based methodology isolates the changes in CD and LLE in specific subbands of the EEG. The methodology is applied to three different groups of EEG signals: 1) healthy subjects; 2) epileptic subjects during a seizure-free interval (interictal EEG); 3) epileptic subjects during a seizure (ictal EEG). The effectiveness of CD and LLE in differentiating between the three groups is investigated based on statistical significance of the differences. It is observed that while there may not be significant differences in the values of the parameters obtained from the original EEG, differences may be identified when the parameters are employed in conjunction with specific EEG subbands. Moreover, it is concluded that for the higher frequency *beta* and *gamma* subbands, the CD differentiates between the three groups, whereas for the lower frequency *alpha* subband, the LLE differentiates between the three groups.**

***Index Terms*—Chaos theory, EEG subbands, electroencephalogram (EEG), epilepsy, wavelet transform.**

I. Introduction

EPILEPSY is a common brain disorder that affects about 1% of the population in the United States and is characterized by intermittent abnormal firing of neurons in the brain [1]. Brain activity in the ictal state (during a seizure) differs significantly from the activity in the normal state with respect to frequency and pattern of neuronal firing. Nevertheless, detection of seizures can be challenging even from a visual inspection of the EEG by a trained neurologist for a variety of reasons such as excessive presence of myogenic artifacts. Prediction of seizures is even more challenging because there is very little confirmed knowledge of the exact mechanism responsible for the seizure. Effective algorithms for automatic seizure detection and prediction can have a far reaching impact on diagnosis and treatment of epilepsy.

In recent years, a few attempts have been reported on seizure detection and prediction from EEG analysis using two different approaches: 1) Examination of the waveforms in the preictal EEG to find events (markers) or changes in neuronal activity such as spikes [2], [3] which may be precursors to seizures; 2) Analysis of the nonlinear spatio-temporal evolution of the EEG signals to find a governing rule as the system moves from a seizure-free to seizure state [4]. Some work has also been reported using artificial neural networks [5] for seizure prediction with wavelet preprocessing [6]. This paper focuses on the second approach using a combination of chaos theory and wavelet analysis. Researchers have performed either chaos or wavelet analysis for nonlinear dynamic analysis of EEGs. To the best of the authors' knowledge no research has been published on an integrated approach and simultaneous application of both chaos theory and wavelets for analysis of EEG records which is the multiparadigm approach advocated and used by the authors in this research.

This research also challenges the assumption that the EEG represents the dynamics of the entire brain as a unified system and needs to be treated as a whole. On the contrary, an EEG is a signal that represents the effect of the superimposition of diverse processes in the brain. Very little research has been done to separately study the effects of these individual processes. Each EEG is commonly decomposed into five EEG subbands: *delta* (0–4 Hz), *theta* (4–8 Hz), *alpha* (8–12 Hz), *beta* (13–30 Hz), and *gamma* (30–60 Hz). There is no good reason why the entire EEG should be more representative of brain dynamics than the individual frequency subbands. In fact, the subbands may yield more accurate information about constituent neuronal activities underlying the EEG and consequently, certain changes in the EEGs that are not evident in the original full-spectrum EEG may be amplified when each subband is analyzed separately. This is a premise of this research.

Iasemidis and Sackellares [7] were among the first to study the nonlinear dynamics of EEG data in patients with temporal lobe epilepsy and in their subsequent studies concluded that the chaos in the brain was reduced in the preictal phase [8], [9]. Bullmore *et al.* [10] performed a quantitative comparison of EEGs corresponding to normal and epileptic brain activity using fractal analysis. Similar findings confirming the reduction in complexity of neuronal firing during the preictal phase were also reported by Elger and Lehnertz [11], [12]. Lopes da Silva *et al.* [13] reported the synchronization of neuronal firing in different parts of the brain during a seizure. Hively *et al.* [14] also proposed additional measures using chi-square statistics and phase space visitation frequency to quantify chaos in EEGs and to detect the transition from nonseizure to epileptic activity.

A major shortcoming of existing seizure detection algorithms is their low accuracy resulting in high missed detection and false alarm rates [15]. A robust methodology is key to accurate seizure detection and prediction. Robustness is generally

Manuscript received July 19, 2004; revised March 8, 2006. *Asterisk indicates corresponding author.*

*H. Adeli is with the Departments of Biomedical Engineering, Biomedical Informatics, Civil and Environmental Engineering and Geodetic Science, Electrical and Computer Engineering, and Neuroscience, The Ohio State University, 470 Hitchcock Hall, 2070 Neil Avenue, Columbus, OH 43210 USA (e-mail: adeli.1@osu.edu).

S. Ghosh-Dastidar is with the Department of Biomedical Engineering, The Ohio State University, Columbus, OH 43210 USA.

N. Dadmehr is at 555 W. Schrock Rd, # 140, Westerville, OH 43081 USA.

Digital Object Identifier 10.1109/TBME.2006.886855

defined as: 1) decreased sensitivity to physiological differences between individuals and inherent inaccuracies in EEGs such as noise and electrode artifacts; 2) increased specificity to the particular disorder of interest, for example temporal lobe epilepsy (TLE). Another disadvantage is the lack of reliable standardized data to test the accuracy of such algorithms. This reduces the statistical significance of the results since most of the EEG analysis reported in the literature is performed on a small number of data sets. In order to obtain a reliable estimate of the efficacy of the epilepsy detection parameters and algorithms, they should be tested on a relatively large number of data sets.

In this paper, a wavelet-chaos methodology is presented for analysis of EEGs and EEG subbands for detection of seizure and epilepsy. It consists of three stages: 1) wavelet analysis; 2) preliminary chaos analysis; 3) final chaos analysis. The methodology is applied to three different groups of EEG signals: 1) healthy subjects; 2) epileptic subjects during a seizure-free interval (interictal EEG); 3) epileptic subjects during a seizure (ictal EEG). Each EEG is decomposed into five constituent EEG subbands: *delta*, *theta*, *alpha*, *beta*, and *gamma* using wavelet-based filters. The nonlinear chaotic dynamics of the original EEGs are quantified in the form of the correlation dimension (CD) and the largest Lyapunov exponent (LLE). Similar to the original EEG, each subband is also subjected to chaos analysis to investigate the isolation of the changes in CD and LLE to specific subbands of the EEG. Subsequently, the effectiveness of CD and LLE in differentiating between the three groups is investigated based on statistical significance of the differences.

II. Chaos Analysis of EEG Signals

A. Measures of Chaos

Nonlinear systems such as EEGs tend to gravitate towards specific regions in phase space known as attractors. The most important representation of an attractor is the governing rule or map that determines how the system evolves forward in time. Two main characteristics in the analysis of an attractor are complexity and chaoticity. Complexity is a measure of the geometric properties of the attractor and is characterized by the magnitude of the attractor dimension which need not be an integer value. For instance, an attractor embedded in a phase space of embedding dimension 2 would typically have a dimension between 1 and 2 [10], [16]–[19]. In this research the CD is used as the measure of attractor complexity because it characterizes the attractor at a fine resolution and is computationally efficient.

The chaoticity of the attractor is a measure of the convergence or divergence of nearby trajectories in phase space. The "butterfly effect" theory of chaos states that in a chaotic system, two points close together in phase space have completely different outcomes. This implies that a divergence in the trajectories suggests chaos in a system and *vice versa*. In this research, the LLE is employed to quantify the attractor chaoticity.

During normal brain activity, the pattern of neuronal firing represented by the EEG signal is less organized and has greater complexity and chaoticity. However, prior to a seizure, the pattern of neuronal firing becomes more organized and is characterized by lower values of the LLE and CD of the chaotic attractor [15], [20]. There are conflicting reports on the values of the CD during a seizure. Hively *et al.* [14] report values of CD greater than 6 during seizure and between 1 and 2.6 otherwise, whereas Iasemidis *et al.* [7] report values in the range of 2 and 3 during seizure.

B. Preliminary Chaos Analysis – Creation of Lagged Phase Space of the EEG Signal

The EEG signal is represented as a time series vector, $\mathbf{X} = \{x_1, x_2, \ldots, x_N\}$ comprised of single voltage readings at various time intervals and expressed as a series of individual data points (single voltage readings by an electrode) where N is the total number of data points and the subscript indicates the time instant. Assuming a selected time lag m, $\mathbf{X_T}$ represents a time series vector that contains all data points in $\mathbf{X}$ from time instant T to $N-m$ (i.e., $x_T, x_{T+1}, \ldots, x_{N-m}$) and $\mathbf{X_{T+m}}$ represents a time series vector that contains all data points in $\mathbf{X}$ from time instant $T+m$ to N (i.e., $x_{T+m}, x_{T+m+1}, \ldots, x_N$), then the graph of $\mathbf{X_{T+m}}$ versus $\mathbf{X_T}$ is known as the pseudo or lagged phase space with lag m and embedding dimension 2. Both $\mathbf{X_T}$ and $\mathbf{X_{T+m}}$ are subsets of $\mathbf{X}$ and contain $N-T-m+1$ data points each. To create the lagged phase space, two parameters must be identified: the optimum lag and the minimum embedding dimension (MED).

To find the optimum lag, the EEG signal is tested for mutual information which is a measure of the extent of overlap between the information contained in $\mathbf{X_T}$ and $\mathbf{X_{T+m}}$. The optimum lag m_0 is termed so because it has to be large enough for $\mathbf{X_T}$ and $\mathbf{X_{T+m}}$ to yield minimal overlapping information without being so large that the number of data points in the signals compared becomes too small. Since the total number of data points in the EEG signal is limited to N, for a given lag m, $\mathbf{X_T}$ and $\mathbf{X_{T+m}}$ each contain $N-m$ data points. If the value of m is too large, then the size of the vectors $\mathbf{X_T}$ and $\mathbf{X_{T+m}}$ becomes very small and some important features may be lost. Varying the value of m yields mutual information coefficients (I_m) for different values of the time lag. The optimum lag is the first local minimum on the graph of I_m versus m.

After the selection of the optimum lag, in the proposed wavelet-chaos algorithm the MED for the EEG signal is estimated using Cao's method [16]. Next, the i^{th} time-delay vector is reconstructed from the EEG signal $\mathbf{X}$ using the optimum lag value, m_0, and the estimated MED, d_M. The reconstructed time delay vector in the lagged phase space has the form $\mathbf{Y}_i(d) = \{x_i, x_{i+m_0}, \ldots, x_{i+m_0(d-1)}\}$ where $i = 1, 2, \ldots, N - m_0(d-1)$, d is the embedding dimension, and x_i is the i^{th} data point in the EEG signal. The underlying principle of this method is that if d is a *true* embedding dimension, then two points that are close to each other in the d-dimensional phase space will remain close in the $d+1$-dimensional phase space. Any two points satisfying the above condition are known as *true* neighbors [16].

The method is applied repeatedly starting with a low value of the embedding dimension d and then increasing it until the number of false neighbors decreases to zero, or equivalently, Cao's embedding function defined as [16]

$$E(d) = \frac{1}{N - m_0 d} \sum_{i=1}^{N-m_0 d} a_i(d) \tag{1}$$

becomes constant. In (1)

$$a_i(d) = \frac{\left\|\mathbf{Y}_i(d+1) - \mathbf{Y}_{n(i,d)}(d+1)\right\|}{\left\|\mathbf{Y}_i(d) - \mathbf{Y}_{n(i,d)}(d)\right\|} \tag{2}$$

where $i = 1, 2, \ldots, N - m_0 d$, and $\mathbf{Y}_{n(i,d)}(d)$ is the nearest neighbor of $\mathbf{Y}_i(d)$ in the d-dimensional space. The proximity of two neighbors for deciding the nearest neighbor is based on a measure of distance computed using the maximum norm function denoted by the $\|*\|$ symbol in (2). The embedding function is modified to model the variation from d to $d+1$ by defining another function, $E1(d) = E(d+1)/E(d)$, which converges to 1 in the case of a finite dimensional attractor [16].

The MED, d_M, is identified from the graph of $E1(d)$ versus d as the value of d at which the value of $E1(d)$ approaches 1. However, in certain cases this may occur even with truly random signals. In order to distinguish deterministic data from truly random signals, another function is defined as $E2(d) = E^*(d+1)/E^*(d)$ where $E^*(d)$ is defined as [16]

$$E^*(d) = \frac{1}{N - m_0 d} \sum_{i=1}^{N - m_0 d} \left| x_{i+m_0 d} - x_{n(i,d)+m_0 d} \right| \tag{3}$$

in which $x_{n(i,d)+m_0 d}$ is the nearest neighbor of $x_{i+m_0 d}$. From an examination of the graph of $E2(d)$ versus d, a constant value of one for $E2(d)$ for different values of d indicates a truly random signal. The signal is found to be deterministic if the value of $E2(d)$ is not equal to 1 for at least one value of d. The embedding dimension for the phase space is set to the MED. The lagged phase space is constructed based on the identified values of the optimum time lag and the embedding dimension.

C. Final Chaos Analysis

In the proposed wavelet-chaos algorithm, the CD is computed using the Takens estimator which states that given a finite signal consisting of $N_C = N - m_0 d_M$ points, named $\mathbf{Y}_1(d_M), \ldots, \mathbf{Y}_{N_C}(d_M)$, there can be a total of $N_C = N - m_0 d_M$ pairwise distances (represented mathematically as $\|x_i - x_j\|$ where $i \neq j$). The CD is directly computed as [17], [21]

$$\upsilon = -\left[\frac{2}{N_C(N_C-1)} \sum_{i=1}^{N_C} \sum_{j=1}^{N_C} \log\left(\frac{|\mathbf{Y}_i(d_M) - \mathbf{Y}_j(d_M)|}{\varepsilon}\right)\right]^{-1} \tag{4}$$

where $\mathbf{Y}_i(d_M)$ and $\mathbf{Y}_j(d_M)$ are the lagged phase space locations of the i^{th} and j^{th} points respectively for the selected embedding dimension d_M, and ε is the radius of the measuring unit.

The number of standard Lyapunov exponents is equal to the embedding dimension of the attractor. For the system to be chaotic, at least one of these exponents should be positive which implies that the LLE ($\lambda_{\max}$) has to be greater than zero. The LLE characterizes the rate of divergence of two neighboring trajectories in the phase space. Trajectory divergence is defined as the distance between two neighboring points in lagged phase space after a given time (known as prediction length). The average trajectory divergence, D_T, of the attractor for a given prediction length, T, is expressed mathematically according to Wolf's method as [22]–[24] as

$$D_T = \frac{1}{N_S} \sum_{i=1}^{N_S} \left| \frac{\mathbf{Y}_{i+T}(d) - \mathbf{Y}'_{i+T}(d)}{\mathbf{Y}_i(d) - \mathbf{Y}'_i(d)_i} \right| \tag{5}$$

where $\mathbf{Y}_i(d)$ and $\mathbf{Y}'_i(d)$ are neighboring points on separate trajectories in the phase space, and $\mathbf{Y}_{i+T}(d)$ is the location of the point that evolved from $\mathbf{Y}_i(d)$ along the trajectory. The prediction length, T, is measured in increments of time used for the EEG signal. The LLE ($\lambda_{\max}$) is then computed as the slope of the graph of the natural logarithm of trajectory divergence, D_T, versus the prediction length, T. This relationship is expressed mathematically as $D_T = D_0 e^{T\lambda_{\max}}$ where D_0 is the initial divergence. In this research, a modification of Wolf's method reported in Iasemidis *et al.* [25] is implemented in which the parameters are adaptively estimated to better account for the nonstationary nature of EEGs.

III. Wavelet-Based EEG subband Decomposition

In order to extract the individual EEG subbands a wavelet filter is employed instead of the traditional Fourier transform because the wavelet transform has the advantages of time-frequency localization, multirate filtering, and scale-space analysis [26], [27]. Wavelet transform uses a variable window size over the length of the signal, which allows the wavelet to be stretched or compressed depending on the frequency of the signal [2], [18], [27]. This results in excellent feature extraction from nonstationary signals such as EEGs. In this research, the discrete wavelet transform (DWT) based on dyadic (powers of 2) scales and positions is used to make the algorithm computationally very efficient without compromising accuracy.

The EEG signal is decomposed into progressively finer details by means of multiresolution analysis using complementary lowpass (H_0) and highpass (H_1) filters (explained further in [2]). After a first level decomposition, two sequences representing the high and low resolution components of the signal are obtained. The low-resolution components are further decomposed into low and high resolution components after a second level decomposition and so on. The multiresolution analysis, using four levels of decomposition, yields five separate EEG subbands which are subjected to subsequent chaos analysis. This process is explained in detail in the next section.

IV. Application and Results

A. Description of the EEG Data Used in the Research

The data used in this research are a subset of the EEG data for both healthy and epileptic subjects made available online by Dr. Ralph Andrzejak of the Epilepsy Center at the University of Bonn, Germany (*http://www.meb.uni-bonn.de/epileptologie/science/physik/eegdata.html*). EEGs from three different groups are analyzed: group H (healthy subjects), group E (epileptic subjects during a seizure-free interval), and group S (epileptic subjects during seizure) are analyzed. The type of epilepsy was diagnosed as temporal lobe epilepsy with the epileptogenic focus being the hippocampal formation. Each group contains

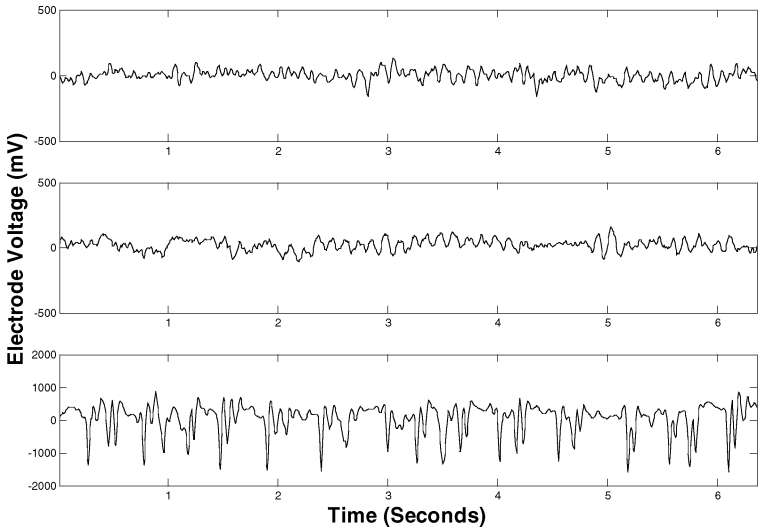

Fig. 1. Sample unfiltered EEGs (0–6 s) for (from top to bottom) Group H (H029), Group E (E037), and Group S (S001).

100 single channel EEG segments of 23.6 sec duration each sampled at 173.61 Hz [28]. As such, each data segment contains $N = 4097$ data points collected at intervals of 1/173.61th of 1 s. Each EEG segment is considered as a separate EEG signal resulting in a total of 300 EEG signals or EEGs. As an example, the first 6 s of three EEGs (signal numbers in parentheses) for groups H (H029), E (E037), and S (S001) are magnified and displayed in Fig. 1.

B. Data Preprocessing and Wavelet Decomposition of EEG Into Subbands

The five primary EEG subbands: *delta*, *theta*, *alpha*, *beta*, and *gamma* span the 0–60 Hz frequency range and higher frequencies are often characterized as noise. Since the sampling frequency of the EEG is 173.61 Hz, according to the Nyquist sampling theorem, the maximum useful frequency is half of the sampling frequency or 86.81 Hz. As such, from a physiological standpoint, frequencies greater than 60 Hz can be classified as noise and discarded. Moreover, unlike the Fourier transform, wavelet decomposition does not allow the extraction of specific frequency bands without additional processing. Consequently, to correlate the wavelet decomposition with the frequency ranges of the physiological subbands, the wavelet filter used in this application requires the frequency content to be limited to the 0–60 Hz band. Due to the abovementioned reasons, the EEG is band-limited to the desired 0–60 Hz range by convolving with a low-pass finite impulse response (FIR) filter. The energy of the frequency band eliminated by the filter is negligible compared with that of the retained band in the range 0–60 Hz.

The band-limited EEG is then subjected to a level 4 decomposition using fourth-order Daubechies wavelet transform. After the first level of decomposition, the EEG signal, $\mathbf{s}$ (0–60 Hz), is decomposed into its higher resolution components, $\mathbf{d_1}$ (30–60 Hz) and lower resolution components, $\mathbf{a_1}$ (0–30 Hz). In the second level of decomposition, the $\mathbf{a_1}$ component is further decomposed into higher resolution components, $\mathbf{d_2}$ (15–30 Hz) and lower resolution components, $\mathbf{a_2}$ (0–15 Hz). Following this process, after four levels of decomposition, the components retained are $\mathbf{a_4}$ (0–4 Hz), $\mathbf{d_4}$ (4–8 Hz), $\mathbf{d_3}$ (8–15 Hz), $\mathbf{d_2}$ (15–30 Hz), and $\mathbf{d_1}$ (30–60 Hz). Reconstructions of these five components using the inverse wavelet transform approximately correspond to the five physiological EEG subbands *delta*, *theta*, *alpha*, *beta*, and *gamma* (Fig. 2). Minor differences in the boundaries between the components compared to those between the EEG subbands are of little consequence due to the physiologically approximate nature of the subbands.

C. Results of Chaos Analysis for a Sample Set of Unfiltered EEGs

The optimum lag, m_0, for each EEG is computed as the first local minimum in the plot of the mutual information coefficient versus the lag time. The values of the optimum lag m_0 for the three EEGs (H029, E037, and S001) were found to be 5, 7, and 4, respectively. The MEDs for the EEGs are computed using Cao's method. The values of the modified embedding function $E1(d)$ in all cases approach 1 indicating chaos in the three sample EEGs obtained from both healthy and epileptic subjects. Additionally, not all values of $E2(d)$ are equal to 1 and therefore the EEGs contain deterministic chaos. Convergence is assumed to be reached when the variation of the values of $\mathrm{E1(d)}$ in three consecutive steps is within 5% of the maximum of all values. The MEDs for the three EEGs (H029, E037, and S001) are obtained to be equal to 7.

The values of CD are obtained using the Takens estimator (4). The radius (ε) is varied from 0%–20% of the size of the lagged phase space. In the case of a very small radius not enough points are captured for the computation, whereas in the case of a large radius most of the available points are captured. Both these situations lead to an incorrect selection of nearest neighbors and yield inaccurate estimates of the CD. By trial and error, it is observed that the method yields fairly consistent estimates of CD within the range of 6%–10% of maximum attractor size with highly variable estimates beyond that range. Therefore, the maximum value of the radius is set to 10% of the size of the lagged phase space. The values of CD for the three EEGs (H029, E037,

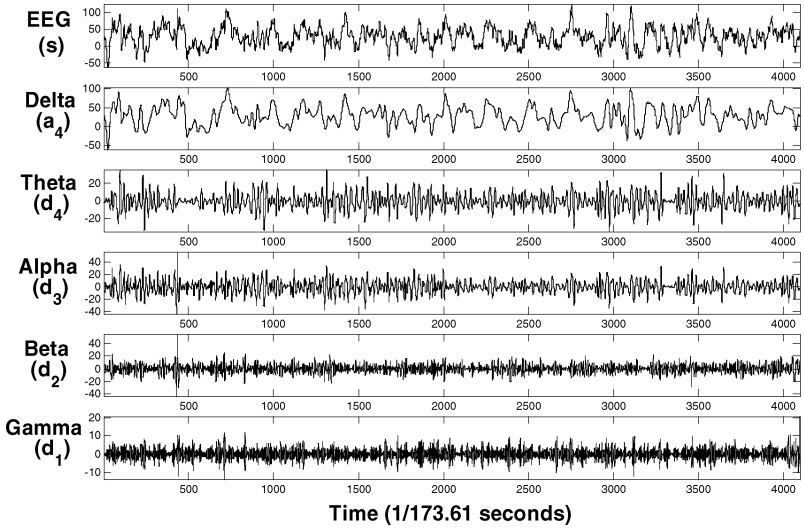

Fig. 2. Level 4 decomposition of the band-limited EEG into five EEG subbands using fourth-order Daubechies wavelet ($\mathbf{s = a_4 + d_4 + d_3 + d_2 + d_1}$).

and S001) are 7.0, 6.8, and 5.5, respectively. The values of the CD are less than or equal to the values for the MED for all three sample EEGs, which is consistent with the theory that the MED should be greater than CD for any chaotic attractor [29].

The values of LLE are computed using the modification of Wolf's method as explained in Iasemidis *et al.* [25]. The values of LLE for the three EEGs (H029, E037, and S001) are 0.074, 0.037, and 0.067, respectively.

D. Statistical Analysis of Results for All EEGs

The chaos analysis presented in the previous section is repeated for all 300 band-limited EEGs (100 from each group H, E, and S) and for all five subbands of each EEG. This is a rather large EEG data set that can yield statistically significant results. The average values and standard deviations of the two parameters, CD and LLE, are computed for the band-limited EEGs and their subbands and summarized in Tables I and II, respectively. It is observed from these results that neither parameter by itself yields a sufficient method for quantification of the differences in the three groups. In some cases the range of values of CD and LLE of one group overlaps the values of another group. This indicates that a simple threshold applied to these parameters is insufficient to distinguish between the groups. Even so, it is clear that some of these reported variations are significant. Also, it should be noted that filtering of the signal alters the parameters employed to find the embedded attractor which may lead to a very different phase space behavior. Consequently, the properties of the phase space and the attractor for the subbands are no longer comparable directly to those for the original band-limited EEG.

From the CD values obtained from the band-limited EEGs (Table I), it is observed that group S (5.3) differs from the other two groups, H (6.9) and E (6.7). However, the CD values for groups H and E do not appear to be significantly different from each other. The low value of CD for group S suggests a lowering of the complexity of the chaotic attractor during a seizure. Examination of the *delta* and *theta* subbands yields very similar values of CD for all three groups, H, E, and S (Table I). The CD values in case of the *alpha* subband for group E (4.7) differs from the other two groups, H (4.0) and S (4.2) which do not appear to differ significantly from each other. This implies that if the *alpha* subband is considered to be a representation of brain dynamics by itself, then the attractor of the *alpha* subband, dubbed *alpha* attractor by the authors, has high complexity in epileptic patients during seizure-free intervals. The CD values for the *beta* and *gamma* subbands show considerable difference between all three groups. It is observed (Table I) that both *beta* and *gamma* attractors have the lowest complexity during a seizure, highest complexity for a healthy subject, and intermediate complexity for an epileptic subject during a seizure-free interval.

From the LLE values obtained from the band-limited EEGs (Table II), it is observed that all three groups, H, E, and S appear to differ from each other. The values suggest that the chaoticity of the chaotic attractor is highest in a healthy subject, lowest in an epileptic subject during a seizure-free state, and intermediate

TABLE I
AVERAGE VALUES OF CD (STANDARD DEVIATION IN PARENTHESIS) FOR BAND-LIMITED EEGS AND EEG SUBBANDS FOR ALL GROUPS

Signal	Group H N=100	Group E N=100	Group S N=100
Band-limited EEG (0-60 Hz)	6.9 (1.4)	6.7 (1.2)	5.3 (1.3)
Delta (0-4 Hz)	5.9 (1.2)	5.7 (1.3)	5.4 (1.4)
Theta (4-8 Hz)	4.0 (0.5)	4.3 (0.8)	4.2 (0.6)
Alpha (8-12 Hz)	4.0 (0.5)	4.7 (1.0)	4.2 (0.8)
Beta (12-30 Hz)	4.5 (0.6)	4.1 (1.1)	3.5 (1.1)
Gamma (30-60 Hz)	3.7 (0.5)	3.1 (1.0)	2.6 (1.0)

TABLE II
AVERAGE VALUES OF LLE (STANDARD DEVIATION IN PARENTHESIS) FOR BAND-LIMITED EEGS AND EEG SUBBANDS FOR ALL GROUPS

Signal	Group H N=100	Group E N=100	Group S N=100
Band-limited EEG (0-60 Hz)	0.089 (0.026)	0.041 (0.015)	0.070 (0.028)
Delta (0-4 Hz)	0.034 (0.007)	0.037 (0.008)	0.043 (0.012)
Theta (4-8 Hz)	0.096 (0.020)	0.082 (0.017)	0.080 (0.016)
Alpha (8-12 Hz)	0.106 (0.019)	0.078 (0.017)	0.086 (0.023)
Beta (12-30 Hz)	0.157 (0.037)	0.159 (0.031)	0.154 (0.033)
Gamma (30-60 Hz)	0.221 (0.064)	0.231 (0.073)	0.226 (0.066)

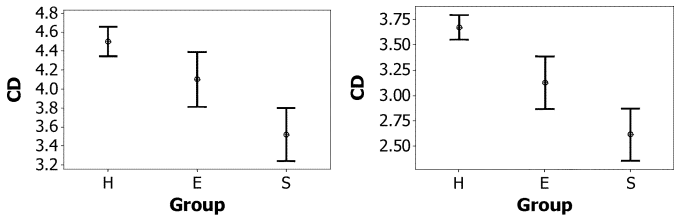

Fig. 3. Confidence interval (confidence level = 99%) plots of CD values for (a) *beta* and (b) *gamma* subbands showing significant differences in CD between all three EEG groups H, E, and S.

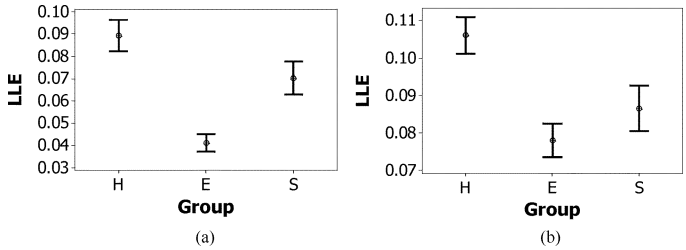

Fig. 4. Confidence interval (confidence level = 99%) plots of LLE values for (a) band-limited EEG and (b) *alpha* subband showing significant differences in LLE between all three EEG groups H, E, and S.

TABLE III
RESULTS OF THE STATISTICAL ANALYSIS SUMMARIZING GROUPS THAT ARE SEPARABLE USING CD AND LLE APPLIED TO THE BAND-LIMITED EEGS AND EEG SUB-BANDS (ANOVA p-VALUES IN PARENTHESIS)

Signal	Groups Differentiated By	
	CD	LLE
Band-limited EEG (0-60 Hz)	S (from E and H) ($p < 0.001$)	H, E, S ($p < 0.001$)
Delta (0-4 Hz)	-	S (from E and H) ($p < 0.001$)
Theta (4-8 Hz)	-	H (from E and S) ($p < 0.001$)
Alpha (8-12 Hz)	E (from H and S) ($p < 0.001$)	H, E, S ($p < 0.001$)
Beta (12-30 Hz)	H, E, S ($p < 0.001$)	-
Gamma (30-60 Hz)	H, E, S ($p < 0.001$)	-

during a seizure. The LLE values for the *alpha* subband show considerable difference between all three groups and the same trend as in the case of the band-limited EEG. The LLE values in case of the *theta* subband for group H (0.096) differs from the other two groups, E (0.082) and S (0.080) which do not appear to differ significantly from each other. This implies that the *theta* attractor has high chaoticity in healthy subjects. Examination of the *delta, beta,* and *gamma* subbands yields very similar values of LLE for all three groups, H, E, and S (Table II).

In the ensuing discussions, one-way analysis of variance (ANOVA) is used for all statistical significance analysis performed at the 99% confidence level. Additionally, the significance of group differences is assessed using the method of Tukey's pairwise differences and the results are summarized in Table III along with p-values. Identical results are obtained using 99% confidence intervals ($\alpha = 0.01$) for both ANOVA and Tukey's method of pairwise differences. These results are consistent with the results discussed thus far in this section. The CD differentiates between all three groups when computed based on the higher frequency *beta* and *gamma* subbands which have an identical pattern of high and low CD values (Fig. 3). Also, the statistical analysis reveals that the CD of the *alpha* subband distinguishes group E from both groups H and S, an observation not evident from Tables I and II. However, the CD for the *alpha* subband shows higher complexity for group E which is different from that noted in *beta* and *gamma* subbands (Table III). This can be the reason why examination of the values of CD for the band-limited EEG differentiates only group S (from both groups E and H) but does not distinguish between groups E and H (Table III). The CD of the lower frequency *delta* and *theta* subbands yields no information at all (Table III).

Unlike the CD, the LLE differentiates between all three groups when computed based on the intermediate frequency *alpha* subband. In case of the lower frequency subbands, the *delta* LLE distinguishes group S (from both groups E and H) and *theta* LLE distinguishes group H (from both groups E and S) (Table III). However, as recorded in Table II, the patterns of high and low LLE values for these subbands are such that the effects do not contradict each other. Consequently, the LLE of the entire band-limited EEG also distinguishes between all three groups (Fig. 4). The LLE of the higher frequency *beta* and *gamma* subbands yields no information at all.

V. CONCLUDING REMARKS

A wavelet-chaos methodology was presented for analysis of EEGs and *delta*, *theta*, *alpha*, *beta*, and *gamma* subbands of EEGs for detection of seizure and epilepsy. Although it is observed that the LLE of the band-limited EEG can potentially distinguish between the three groups of subjects, it cannot be concluded with certainty that it will. If based on a large number of EEG segments the average values of the LLE or CD for the three groups are distinctly different then better seizure detection can be expected but not guaranteed. Since the EEG is an overall representation of brain dynamics, it opens up the possibility that the observed changes in the parameters quantifying chaos in the band-limited EEG are actually the result of the superimposition of multiple processes underlying the EEG.

One method of studying these underlying processes is to study the component physiological subbands of the EEG which can be assumed to represent these processes at a finer level. The decomposition of the original EEG into its five constituent subbands alters the original phase space and leads to new phase spaces that do not necessarily correspond directly to that of the original EEG. In other words, each subband is assumed to have its own chaotic attractor. When the statistical analysis is based on the entire band-limited EEG, one may conclude that only the LLE (and not the CD) may be used as a discriminating parameter between the three groups. However, when the statistical analysis is performed on the EEG subbands, it is observed that the CD used within certain physiological subbands may also be employed to distinguish between all three groups. Therefore, it is concluded that changes in the dynamics are not spread out equally across the spectrum of the EEG, but instead, are limited to certain frequency bands.

The availability of multiple potential discriminating parameters will result in increased accuracy of real-time EEG epilepsy and seizure detection systems that will be explored in future work.

REFERENCES

[1] Seizures and Epilepsy: Hope through Research National Institute of Neurological Disorders and Stroke (NINDS), Bethesda, MD, 2004 [Online]. Available: http://www.ninds.nih.gov/health_and_medical/pubs/seizures_and_epilepsy_htr. htm

[2] H. Adeli, Z. Zhou, and N. Dadmehr, "Analysis of EEG records in an epileptic patient using wavelet transform," *J. Neurosci. Meth.*, vol. 123, no. 1, pp. 69–87, 2003.

[3] P. J. Durka, "From wavelets to adaptive approximations: Time-frequency parameterization of EEG," *BioMedical Engineering OnLine*, vol. 2, no. 1, pp. 1(1)–1(30), 2003 [Online]. Available: http://www.biomedical-engineering-online.com/

[4] L. D. Iasemidis, L. D. Olson, J. C. Sackellares, and R. S. Savit, "Time dependencies in the occurrences of epileptic seizures: A nonlinear approach," *Epilepsy Res.*, vol. 17, pp. 81–94, 1994.

[5] H. Adeli and S. L. Hung, *Machine Learning – Neural Networks, Genetic Algorithms, and Fuzzy Sets*. New York: Wiley, 1995.

[6] Petrosian, D. Prokhorov, R. Homan, R. Dascheiff, and D. Wunsch, II, "Recurrent neural network based prediction of epileptic seizures in intra- and extracranial EEG," *Neurocomputing*, vol. 30, no. 1–4, pp. 201–218, 2000.

[7] L. D. Iasemidis and J. C. Sackellares, "The temporal evolution of the largest Lyapunov exponent on the human epileptic cortex," in *Measuring Chaos in the Human Brain*, D. W. Duke and W. S. Pritchard, Eds. Singapore: World Scientific, 1991, pp. 49–82.

[8] L. D. Iasemidis, D. S. Shiau, J. C. Sackellares, and P. M. Pardalos, "Transition to epileptic seizures: Optimization," in *DIMACS Series in Discrete Mathematics and Theoretical Computer Science*. Providence, RI: American Mathematical Society, 2000, vol. 55, pp. 55–74.

[9] L. D. Iasemidis, D. S. Shiau, W. Chaovalitwongse, J. C. Sackellares, P. M. Pardalos, J. C. Principe, P. R. Carney, A. Prasad, B. Veeramani, and K. Tsakalis, "Adaptive epileptic seizure prediction system," *IEEE Trans. Biomed. Eng.*, vol. 50, no. 5, pp. 616–627, May 2003.

[10] E. Bullmore, M. Brammer, G. Alarcon, and C. Binnie, "A new technique for fractal analysis applied to human, intracerebrally recorded, ictal electroencephalographic signals," in *Chaos in Medicine: Source Readings*, R. T. Sataloff and M. Hawkshaw, Eds. San Diego, CA: Singular Publishing Group, 1992, pp. 295–298.

[11] C. E. Elger and K. Lehnertz, "Ictogenesis and chaos," in *Epileptic Seizures and Syndromes*, P. Wolf, Ed. London, U.K.: Libbey, 1994, pp. 547–552.

[12] ——, "Seizure prediction by non-linear time series analysis of brain electrical activity," *Eur. J. Neurosci.*, vol. 10, no. 2, pp. 786–789, 1998.

[13] F. H. L. da Silva, J. P. Pijn, and W. J. Wadman, "Dynamics of local neuronal networks: Control parameters and state bifurcations in epileptogenesis," *Prog. Brain Res.*, vol. 102, pp. 359–370, 1994.

[14] L. M. Hively, P. C. Gailey, and V. A. Protopopescu, "Detecting dynamical change in nonlinear time series," *Phys. Lett. A*, vol. 258, no. 2–3, pp. 103–114, 1999.

[15] L. D. Iasemidis, "Epileptic seizure prediction and control," *IEEE Trans. Biomed. Eng.*, vol. 50, no. 5, pp. 549–558, May 2003.

[16] L. Cao, "Practical method for determining the minimum embedding dimension of a scalar time series," *Physica D*, vol. 110, no. 1–2, pp. 43–50, 1997.

[17] G. P. Williams, *Chaos Theory Tamed*. Washington, D.C.: Nat. Acad. Press, 1997.

[18] X. Jiang and H. Adeli, "Fuzzy clustering approach for accurate embedding dimension identification in chaotic time series," *Integr. Comput.-Aided Eng.*, vol. 10, no. 3, pp. 287–302, 2003.

[19] S. V. Notley and S. J. Elliott, "Efficient estimation of a time-varying dimension parameter and its application to EEG analysis," *IEEE Trans. Biomed. Eng.*, vol. 50, no. 5, pp. 594–602, May 2003.

[20] B. Litt and J. Echauz, "Prediction of epileptic seizures," *Lancet Neurol.*, vol. 1, no. 1, pp. 22–30, 2002.

[21] S. Borovkova, R. Burton, and H. Dehling, "Consistency of the takens estimator for the correlation dimension," *Ann. Appl. Probab.*, vol. 9, no. 2, pp. 376–390, 1999.

[22] A. Wolf, J. B. Swift, H. L. Swinney, and J. A. Vastano, "Determining Lyapunov exponents from a time series," *Physica D*, vol. 16, pp. 285–317, 1985.

[23] M. T. Rosenstein, J. J. Collins, and C. J. De Luca, "A practical method for calculating largest Lyapunov exponents from small data sets," *Physica D*, vol. 65, no. 1–2, pp. 117–134, 1993.

[24] R. C. Hilborn, *Chaos and Nonlinear Dynamics: An Introduction for Scientists and Engineers*. Oxford, U.K.: Oxford Univ. Press, 2001.

[25] L. D. Iasemidis, J. C. Principe, and J. C. Sackellares, "Measurement and quantification of spatiotemporal dynamics of human epileptic seizures," in *Nonlinear Biomedical Signal Processing*, M. Akay, Ed. Piscataway, NJ: Wiley-IEEE Press, 2000, vol. II, pp. 294–318.

[26] Daubechies, *Ten Lectures on Wavelets*. Philadelphia, PA: SIAM, 1992.

[27] S. G. Mallat, "A theory for multiresolution signal decomposition: the wavelet representation," *IEEE Trans. Pattern Anal. Mach. Intell.*, vol. 11, no. 7, pp. 674–693, Jul. 1989.

[28] R. G. Andrzejak, K. Lehnertz, C. Rieke, F. Mormann, P. David, and C. E. Elger, "Indications of non-linear deterministic and finite dimensional structures in time series of brain electrical activity: Dependence on recording region and brain state," *Phys. Rev. E*, vol. 64, no. 6, pp. (061907)1–8, 2001.

[29] K. Natarajan, R. U. Acharya, F. Alias, T. Tiboleng, and S. K. Puthusserypady, "Nonlinear analysis of EEG signals at different mental states," *BioMedical Engineering OnLine*, vol. 3, no. 3, pp. 3(1)–3(11), 2004 [Online]. Available: http://www.biomedical-engineering-online.com/

Hojjat Adeli (M'94) received the Ph.D. degree from Stanford University, Stanford, CA, in 1976.

He is Professor of Civil and Environmental Engineering and Geodetic Science, Aerospace Engineering, Biomedical Engineering, Biomedical Informatics, Electrical and Computer Engineering, and Neuroscience, The Ohio State University, Columbus. He is also the holder of Lichtenstein Professorship. He has authored over 400 research and scientific publications in various fields of computer science, engineering, and applied mathematics since 1976. His research has been published in 72 different journals. He has authored 11 books including *Machine Learning – Neural Networks*, *Genetic Algorithms*, and *Fuzzy Systems* (Wiley, 1995); *Wavelets in Intelligent Transportation Systems* (Wiley, 2005). He has also edited 12 books. He is the Founder and Editor-in-Chief of the international research journals *Computer-Aided Civil and Infrastructure Engineering* and *Integrated Computer-Aided Engineering*. He is also the Editor-in-Chief of the *International Journal of Neural Systems*.

In 1998, Dr. Adeli received the Distinguished Scholar Award from The Ohio State University "*in recognition of extraordinary accomplishment in research and scholarship*." In 2005, he was elected Honorary Member of American Society of Civil Engineers "*for wide-ranging, exceptional, and pioneering contributions to computing in many civil engineering disciplines and extraordinary leadership in advancing the use of computing and information technologies in civil engineering throughout the world*."

Samanwoy Ghosh-Dastidar was born in New Delhi, India, in 1976. He studied civil engineering at the University of Roorkee, Roorkee, India, and received the B.E. degree in 1997. He received the M.S. degree in civil engineering from The Ohio State University, Columbus, in 2002. He is currently working towards the Ph.D. degree in biomedical engineering at The Ohio State University.

His research interests include mathematical modeling of dynamic systems, signal and image processing, data mining, artificial neural networks and non-linear (chaos) analysis. Current areas of application include epilepsy diagnosis, detection and prediction of epileptic seizures and early detection of Alzheimer's disease. His previous areas of interest include intelligent transportation systems.

Nahid Dadmehr received the M.D. degree from the University of Tehran, Tehran, Iran, in 1979. Subsequently, she did her medical residency and fellowship at The Ohio State University, Columbus.

She has been practicing in central Ohio since 1991 as a board-certified neurologist. Her research has been published in several journals including the *Clinical Electroencephalography, Electroencephalography and Clinical Neurophysiology*, *Neurology*, and the *Journal of Neuroscience Methods*.